

Imaging lipid lateral organization in membranes with C-laurdan in a confocal microscope^S

Martín M. Dodes Traian,^{*,†} F. Luis González Flecha,[†] and Valeria Levi^{1,*}

Departamento de Química Biológica,* Facultad de Ciencias Exactas y Naturales, Universidad de Buenos Aires, Ciudad Universitaria, CP 1428 Ciudad de Buenos Aires, Argentina; and Laboratorio de Biofísica Molecular,[†] Instituto de Química y Fisicoquímica Biológicas, Universidad de Buenos Aires, CONICET, Buenos Aires, Argentina

Abstract Lateral organization of biological membranes is frequently studied using fluorescence microscopy. One of the most widely used probes for these studies is 2-dimethylamino-6-lauroyl-naphthalene (laurdan). The fluorescence of this probe is sensitive to the environment polarity, and thus laurdan reports the local penetration of water when inserted in membranes. Unfortunately, this probe can only be used under two-photon excitation due to its low photostability. This is a very important limitation, because there are not too many laboratories with capability for two-photon microscopy. In this work, we explored the performance of 6-dodecanoyl-2-[*N*-methyl-*N*-(carboxymethyl)amino]naphthalene (C-laurdan), a carboxyl-modified version of laurdan, for imaging biological membranes using a conventional confocal microscopy setup. We acquired generalized polarization (GP) images of C-laurdan inserted in giant unilamellar vesicles composed of binary mixtures of lipids and verified that the probe allows observing the coexistence of different phases. We also tested the performance of the probe for measurement with living cells and registered GP images of melanophore cells labeled with C-laurdan in which we could observe highly ordered regions such as filopodia. **These findings show that C-laurdan can be successfully employed for studies of membrane lateral organization using a conventional confocal microscope and can open the possibility of studying a wide variety of membrane-related processes.**—Dodes Traian, M. M., F. L. González Flecha, and V. Levi. **Imaging lipid lateral organization in membranes with C-laurdan in a confocal microscope.** *J. Lipid Res.* 2012. 53: 609–616.

Supplementary key words generalized polarization • lipid phases • confocal microscopy

Our knowledge of the organization and function of biological membranes has changed from the original model of Singer and Nicholson. It is now well accepted that membrane components are not randomly organized but are

assembly-forming domains of different compositions, sizes, and dynamics that are essential for the functionality of the membrane (1). Particularly important are lipid rafts, which are small (10–200 nm), heterogeneous, and highly dynamic sterol- and sphingolipid-enriched domains that compartmentalize cellular processes. Small rafts can sometimes be stabilized to form larger platforms through protein–protein and protein–lipid interactions (2, 3). Recent works have demonstrated that these assemblies play key roles in processes such as signaling in immunological synapses (4, 5), membrane trafficking (6, 7), and viral infection cycles (8–10).

To understand the physical basis of cell membrane organization and its relation to functionality, several artificial systems, such as small unilamellar vesicles (SUVs) and large unilamellar vesicles, with mean diameters of 30 nm and 120 nm, respectively (11), multilamellar vesicles (12), supported bilayers (13, 14), and giant unilamellar vesicles (GUVs) (15) have been used. GUV sizes range between 10 and 50 μ m, and thus their curvatures are very similar to those of cells. Moreover, they can be easily imaged in microscopes, allowing their study as individual liposomes (16). The advantage of these model systems is that their composition can be manipulated and thus it is possible to characterize their properties, including the potential formation of phases with different physical properties.

One of the key tools widely used for studying the fluidity of lipid membranes is the fluorescent probe 2-dimethylamino-6-lauroyl-naphthalene (laurdan). This

Abbreviations: C-laurdan, 6-dodecanoyl-2-[*N*-methyl-*N*-(carboxymethyl)amino]naphthalene; DIC, differential interference contrast; DOPC, 1,2-dioleoyl-*sn*-glycero-3-phosphocholine; DPPC, 1,2-dipalmitoyl-*sn*-glycero-3-phosphocholine; GP, generalized polarization; GUV, giant unilamellar vesicle; laurdan, 2-dimethylamino-6-lauroyl-naphthalene; MbCD, methyl- β -cyclodextrin; NA, Numerical Aperture; POPC, 1-palmitoyl-2-oleoyl-*sn*-glycero-3-phosphocholine; Rho-DOPE, lissamine rhodamine B 1,2-dioleoyl-*sn*-glycero-3-phosphocholine; Rho-DPPE, lissamine rhodamine B 1,2-dipalmitoyl-*sn*-glycero-3-phosphocholine; SPM, brain sphingomyelin; SUV, small unilamellar vesicle; Tm, midpoint temperature of phase transition.

¹To whom correspondence should be addressed.

e-mail: vlevi12@gmail.com

^S The online version of this article (available at <http://www.jlr.org>) contains supplementary data in the form of five figures.

This research was supported by ANPCyT (PICT 2010-1876, PICT 2008-1104), PME2006-00563, and UBACyT (20020090200201 and 20020100100048). L.G.F. and V.L. are members of CONICET.

Manuscript received 11 October 2011 and in revised form 1 December 2011.

Published, JLR Papers in Press, December 19, 2011

DOI 10.1194/jlr.D021311

fluorescent molecule has exquisite photophysical properties that make it an almost ideal probe to sense changes in the lipid organization under different conditions (17, 18). Laurdan shows spectral sensitivity to the polarity of its environment, presenting an ~50 nm red shift of its emission spectra in polar solvents (18). Because loosely packed membranes present a higher penetration of water molecules, the emission spectra of laurdan in these membranes is red-shifted with respect to that observed in ordered membranes. Indeed, several studies have shown that laurdan spectroscopic properties reflect local water penetration in the bilayer (18, 19). For these reasons, this probe has been extensively used for the characterization of lipid domains in artificial systems and is now increasingly used to study membrane heterogeneity in living cells (see Ref. 20).

One of the main drawbacks of laurdan is that it rapidly photobleaches under one-photon excitation conditions, determining that it can only be used in two-photon excitation microscopy (21). This is a very important limitation, because there are not too many laboratories with capability for two-photon microscopy, given the elevated cost of these microscopes.

Recently Kim et al. (22) have synthesized a new fluorescent probe, 6-dodecanoyl-2-[*N*-methyl-*N*-(carboxymethyl) amino]naphthalene (C-laurdan), designed for imaging and sensing lipid organization in membranes.

C-laurdan fluorescence is very sensitive to its environment, showing a gradual bathochromic shift with the polarity of the solvent. This behavior is similar to that observed for laurdan, with the exception that the fluorescence spectrum of the latter probe in water is more shifted to the blue than expected if only considering the solvent polarity (22). Also, C-laurdan presents enhanced photostability under two-photon excitation and higher water solubility than laurdan due to the fact that one of the methyl groups of the dimethylamine moiety of laurdan was replaced by a carboxylic group in C-laurdan (22). These properties make C-laurdan an extremely useful probe for studying lipid membrane properties, and thus it is starting to be used in studies of membrane organization in living cells (22, 23).

In this work, we demonstrate that C-laurdan can be successfully used for imaging lipid organization in either artificial or natural membranes using a conventional confocal microscope setup. We believe that the use of this probe under one-photon excitation will expand the possibilities of studying a wide variety of membrane-related biological processes.

MATERIALS AND METHODS

Reagents

1,2-Dipalmitoyl-*sn*-glycero-3-phosphocholine (DPPC) was purchased from Sigma Aldrich (St. Louis, MO), and 1-palmitoyl-2-oleoyl-*sn*-glycero-3-phosphocholine (POPC) was obtained from Avanti Lipids (Alabaster, AL). Brain sphingomyelin (SPM) and 1,2-dioleoyl-*sn*-glycero-3-phosphocholine (DOPC) were kindly provided by Dr. Dolores Carrer (INIMEC, Córdoba, Argentina).

Lissamine rhodamine B 1,2-dipalmitoyl-*sn*-glycero-3-phosphoethanolamine (Rho-DPPE) and laurdan were purchased from Molecular Probes (Eugene, OR). Methyl- β -cyclodextrin (MbCD) was kindly provided by Dr. Alejandra Tricerri (INIBIOLP; La Plata University, Argentina) and C-laurdan was kindly supplied by Prof. Bong Rae Cho (Department of Chemistry, Korea University; Korea).

Small unilamellar vesicles preparation

Small unilamellar vesicles (SUVs) were prepared as described previously (24) with some modifications. Briefly, DPPC was dissolved in CH₂Cl₂, dried under a stream of N₂ and then resuspended in PBS buffer (pH 7.4). This preparation was heated above the transition temperature of the lipid (41.3°C) (25) and then sonicated for 15 min.

Fluorescence spectroscopy measurements

Steady-state emission spectra were acquired in a Jasco FP-6500 spectrofluorimeter (Jasco; Tokyo, Japan) equipped with a Jasco ETC-273T peltier temperature controller (Tokyo, Japan). Excitation and emission slits were set to 3 nm. Samples were heated in 0.2°C intervals and were allowed to equilibrate for 90 s at each temperature before acquiring the spectra. The excitation wavelengths were 356 nm (laurdan) and 405 nm (C-laurdan).

The generalized polarization (GP) of laurdan and C-laurdan was calculated as,

$$GP = \frac{I_{440} - I_{490}}{I_{440} + I_{490}} \quad (Eq. 1)$$

where I_{440} and I_{490} are the emission intensities at 440 and 490 nm, respectively.

Generation of GUVs

GUVs were generated by the electroformation method (26) in a specially designed chamber (16). Briefly, 10 μ l of a solution of the selected lipids (0.3 mg/ml) in CH₂Cl₂ was spread over the Pt electrodes and dried for 1 h under vacuum. The observation chamber was filled with bidistilled water previously heated above the highest transition temperature of the lipid species present in the sample. A sine function (3V, 10 Hz) was applied to the electrodes for 30 min to generate the GUVs. C-laurdan was added after GUV formation prediluted in DMSO (100 μ M) to yield a probe-lipid ratio of 1:300. Rho-DPPE was premixed with the lipids at a ratio of 1:800 before GUV electroformation.

Confocal microscopy measurements and GP determinations

GUV observations were done in an Olympus FV-1000 confocal microscope. The excitation source was a solid diode laser at 405 nm (average power at the sample, 5 μ W). The laser light was reflected by a dichroic mirror (DM405/473) and focused through an Olympus UPlanSApo 60 \times oil immersion objective (Numerical Aperture = 1.35) onto the sample. Fluorescence of C-laurdan was collected by the same objective, passed through the pinhole, and split with a dichroic mirror into two independent spectral detectors set to simultaneously collect fluorescence in the range 415–455 nm and 490–530 nm (channels 1 and 2, respectively).

For three-channel measurements of C-laurdan and Rho-DPPE, the excitation sources were the 405 nm and 559 nm lasers, and the corresponding dichroic mirror (DM405/473/559) was used. Fluorescence was collected in the spectral detectors 1 and 2 as mentioned above, and the third channel of the confocal microscope was set to simultaneously collect fluorescence in the range 575–675 nm. The photomultipliers were set in the photon-counting detection mode.

To avoid artifacts on GP calculation due to the probe photoselection observed when exciting the probe with a linearly polarized laser (27, 28), we inserted below the objective the Nomarski prism included in the differential interference contrast (DIC) slot of the confocal microscope that is normally used for DIC measurements. This setup generates two laterally shifted and partially overlapped excitation volumes with orthogonal polarizations (29). This configuration slightly decreases the image resolution (30) but removes the photoselection-induced artifacts (see supplementary Fig. 1) that may affect GP calculation.

Image processing

GP images were obtained from images collected at the confocal microscope, calculating GP for every pixel of the images,

$$GP = \frac{I_{415-455} - G \times I_{490-530}}{I_{415-455} + G \times I_{490-530}} \quad (Eq. 2)$$

where $I_{415-455}$ and $I_{490-530}$ correspond to the fluorescence collected in channels 1 and 2, respectively.

The G factor for these measurements was determined using a solution 10 μ M C-laurdan in DMSO following a procedure similar to that described previously (22).

GP values at cellular membranes were calculated using a Matlab routine that converts a GP image to a binary image according to a threshold value that allows discriminating the cells from the background. The routine then creates a mask with a width of two pixels around the border of the cells in the binary image, which is then applied to the original GP image to identify pixels corresponding to the cell membrane and then extract the GP value.

Melanophores cell culture and imaging

Immortalized *Xenopus laevis* melanophores were cultured as described (31). For microscopy measurements, cells were grown for 2 days on 25 mm round coverslips and incubated with 5 μ M laurdan or C-laurdan for 30 min. Before observation, the coverslips were washed with PBS and mounted in a custom-made chamber. Confocal imaging of cells labeled with C-laurdan or laurdan was performed as described before using an average laser power at the sample of 2 μ W.

RESULTS

Spectroscopic observation of phase transitions of lipids using C-laurdan

To explore the response of C-laurdan to changes in lipid packing, we used the probe to follow the thermotropic behavior of SUVs of DPPC. The temperature-induced phase transitions of this phospholipid have been well characterized using different techniques (25), and thus this assay allows us to explore the performance of C-laurdan in known conditions.

C-laurdan was incorporated into liposomes up to a probe-lipid ratio of \sim 1:800 (0.4 mM phospholipids and 0.5 μ M probe) and incubated for 1 h to ensure complete partitioning of the probe to the vesicles. The emission spectra of the probe were acquired and analyzed as described in MATERIALS AND METHODS.

The inset in **Fig. 1** shows the fluorescence spectrum of C-laurdan at temperatures below and above the characteristic temperature of transition to the liquid crystalline phase ($T_m = 41.3 \pm 2.5^\circ\text{C}$) (25). As expected, the spectrum

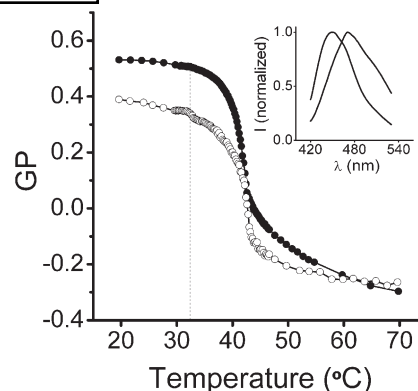


Fig. 1. Thermotropic behavior of DPPC vesicles studied by laurdan (filled circles) and C-laurdan (open circles) generalized polarization. The samples were heated in intervals of 0.2°C and allowed to equilibrate for 90 s at each temperature before acquiring the fluorescence spectrum. The generalized polarization at each temperature was calculated using equation 1. The dashed line shows approximately the temperature for DPPC pretransition (gel to ripple). Inset: Fluorescence spectrum of C-laurdan at 30°C and 60°C (black and gray lines, respectively).

obtained at high temperatures is red-shifted due to the increment of water penetration into the membrane. The intensity of the probe also decreased with the temperature (not shown).

To quantitatively analyze this behavior, we calculated the GP of C-laurdan (equation 1) as a function of the temperature. GP is a function widely used to quantify the spectral behavior of laurdan in artificial and natural membranes, because it can be correlated to the local lipid packing and membrane fluidity (32, 33). High GP values are obtained when the probe spectrum is blue-shifted and thus indicates higher order in the bilayer and low water penetration. Figure 1 shows that the GP of C-laurdan slowly decreased with the temperature until approaching the temperature expected for the transition to the liquid crystalline phase. At this temperature, GP abruptly decreased and continued diminishing with a smaller slope once the transition was completed. We calculated T_m from the experimental data obtaining a value of $41.7 \pm 0.8^\circ\text{C}$, which is not significantly different from that reported previously (25).

To compare the sensitivity of C-laurdan and laurdan to changes in lipid order, we repeated the study described before using laurdan instead of C-laurdan. Figure 1 shows that both probes accurately sensed the phase transition. Interestingly, C-laurdan also allowed sensing the characteristic pretransition from gel to rippled phase described for this phospholipid at $34.4 \pm 2.5^\circ\text{C}$ (25), which could not be observed using laurdan. The temperature determined for this pretransition in our experimental conditions was 32.8°C . Because this transition involves a rearrangement of the phospholipid headgroups (25), this result suggests that the probe preferentially locates near the DPPC headgroups probably via interaction of the carboxylic moiety of C-laurdan with water molecules. In this direction, previous works showed that the pretransition can also be sensed with the fluorescent probe Prodan, which has also been

proposed to locate at the interface (18). This hypothesis agrees with Kim et al. (22), who suggested that the interaction between the carboxyl group of C-laurdan and water molecules at the bilayer interface also decreases the degree of freedom of the fluorescent probe.

To test this hypothesis, we analyzed the behavior of C-laurdan inserted into DPPC liposomes in a buffer at pH 5.6, a pH value significantly lower than the pKa expected for the carboxylic group of this probe (pKa = 6.4) (22). We verified that while the probe could successfully sense the main transition to the liquid crystalline phase, the pretransition could not be observed at this pH (see supplementary Fig. II). It is important to mention that it has been reported that the thermotropic behavior of DPPC is not affected in this pH range (25). This result suggests that the protonated carboxylic group loosely interacts with water molecules at the interface. Moreover the GP value of C-laurdan below T_m was higher at pH 5.6 than at pH 7.4, also suggesting that the probe is probably inserted deeper into the membrane at the acidic pH.

C-laurdan GP measurements in GUVs

Kim et al. (22) showed that C-laurdan presents a higher absorption cross-section with respect to laurdan, in addition to a higher photostability. Both enhanced properties made us hypothesize that C-laurdan could be also brighter and more photostable under one-photon excitation conditions.

To assess this hypothesis, we generated by electroformation GUVs of DPPC:POPC 1:1 including C-laurdan at a 1:300 probe-lipid ratio and observed them at different temperatures in a confocal microscope.

Figure 2 shows that the fluorescence of the probe incorporated in GUVs is clearly detected under regular imaging conditions. We registered simultaneous images of the GUVs using two spectral detectors set in the range 415–455 nm and 490–530 nm (channels 1 and 2, respectively) and calculated

GP images from these measurements. **Figure 2C, D** shows that GP values along the vesicle are homogenous above the T_m ($33.7 \pm 0.2^\circ\text{C}$, see supplementary Fig. III). In contrast, GP images of GUVs at temperatures near T_m clearly show the coexistence of lipid domains with different average GP values.

To correlate the GP measurements of C-laurdan with the properties of the lipid phases, we generated GUVs of DPPC-POPC 1:1 including in the preparation both C-laurdan and Rho-DPPE. This last probe has been extensively used in fluorescence microscopy studies to image lipid domains (34–36) and has been shown to preferentially partition into the fluid phase in a very similar binary system composed of DPPC-DOPC 1:1 (37).

Figure 3 shows that Rho-DPPE is clearly excluded from those domains presenting high GP values of C-laurdan, supporting that these regions probably correspond to gel-like domains. In agreement with this hypothesis, Shoemaker and Vanderlick (38) showed that the mechanical properties of nonfluorescent domains obtained in GUVs composed of DPPC-POPC 6:4 and labeled with lissamine rhodamine B 1,2-dioleoyl-*sn*-glycero-3-phosphocholine (Rho-DOPE) are those expected for gel domains.

To assay whether C-laurdan allows detecting phase separation in GUVs of “raft-forming” lipid mixtures, we generated GUVs composed of DOPC-SPM-Chol 2:2:1 and labeled them with C-laurdan and Rho-DPPE. Supplementary Fig. IV shows that Rho-DPPE colocalized with low GP domains, showing that C-laurdan GP efficiently senses liquid-ordered phases coexisting with liquid-disordered domains. Importantly, the probe Rho-DPPE used in our study behaves as Rho-DOPE and partitions into the liquid-disordered phase (39).

Imaging lipid order in cells with C-laurdan

To further explore the potential uses of C-laurdan for studies of lipid order in biological membranes and compare

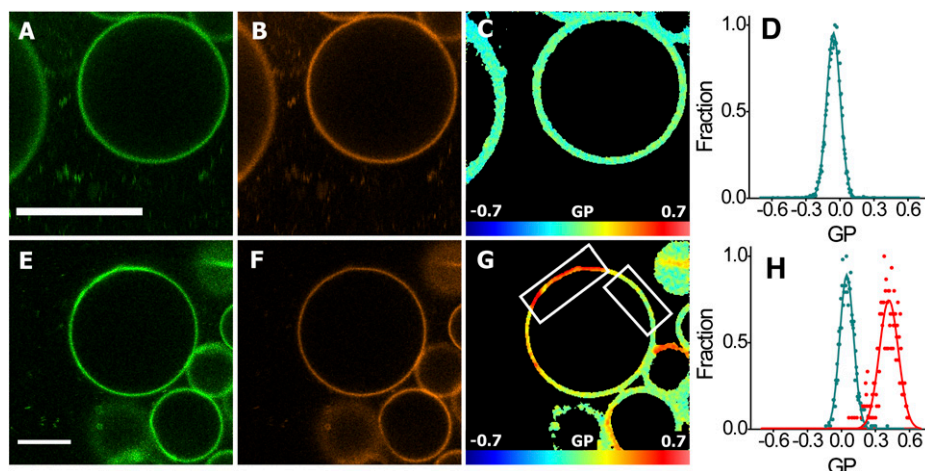


Fig. 2. Observing phase transitions in GUVs with C-laurdan in a confocal microscope. GUVs of DPPC-POPC 1:1 were electroformed at 55°C in the presence of C-laurdan and slowly cooled. GUVs were imaged under the conditions described in MATERIALS AND METHODS at 51.3°C (A–D) and 35.7°C (E–H), registering the fluorescence of the probe at channels 1 (A, E) and 2 (B, F) of the microscope. GP images were obtained from these images using equation 2 (C–G) and were used to calculate the GP distribution of the whole GUV (D) or of regions of the vesicle corresponding to the gel and fluid phases, which are marked with rectangles (H). Bar = 10 μm .

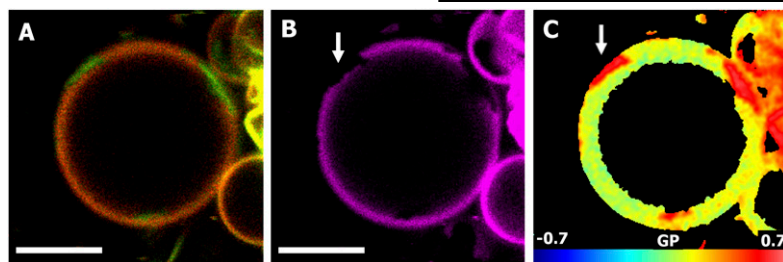


Fig. 3. Characterization of lipid phases with C-laurdan-generalized polarization. GUVs of DPPC-POPC 1:1 were electroformed at 55°C in the presence of C-laurdan and Rho-DEPE. GUVs were observed in the confocal microscope at 27°C, registering simultaneously the fluorescence of C-laurdan (A, composite image channels 1 and 2 are shown in red and green, respectively) and of Rho-DEPE (B), and GP images were calculated from the C-laurdan images (C). The arrows show a region of the GUV corresponding to a high-GP domain and low Rho-DEPE fluorescence. Bar = 10 μm.

its performance with that of laurdan, we acquired images of *X. laevis* melanophore cells labeled with laurdan or C-laurdan as described in MATERIALS AND METHODS. **Figure 4** shows that the fluorescence intensity obtained for C-laurdan-labeled cells is significantly higher than that obtained for laurdan-stained cells, which fluorescence was similar to the autofluorescence (not shown).

Figure 5 shows different slices of a z-scan of GP images and the 3-dimensional reconstruction of the cellular GP obtained for a representative live melanophore cell labeled with C-laurdan. The cell presents regions with significantly different GP values and therefore with different lipid fluidity, as was also verified in a wide variety of cell lines labeled with laurdan and imaged with two-photon excitation microscopes (40). Although C-laurdan labeling membranes within the cell interior presents GP values in the range -0.15 – 0 , the average GP at the plasma membrane was 0.16 . Moreover, the filopodia clearly seen in the images present high GP values of ~ 0.26 , which agree well with the observation of Gaus et al. (40), suggesting that these cellular regions present high

lipid order. On the other hand, we also observed micrometer-sized domains of high GP values in regions of the basal membranes of cells that are in direct contact with the glass substratum. These domains could be focal adhesions, because these regions present high GPs, as was recently demonstrated (41).

Importantly, we measured the intensity of the sample after the acquisition of the z-stack and observed that the average intensity was $\sim 92\%$ of the initial value, showing that the photostability of C-laurdan is adequate for studies requiring repetitive imaging of the sample.

To assay whether C-laurdan can sense changes in the fluidity of the cellular membrane, we studied the effects of MbCD on the membrane properties of *X. laevis* melanophores by measuring C-laurdan GP. Cyclodextrins are extensively used to remove cholesterol from artificial and natural membranes (see Ref. 42), and their effects on membrane properties have been explored using laurdan GP analysis. It has been shown that MbCD increases the fluidity of biological membranes as assessed by a significant reduction of laurdan GP (43).

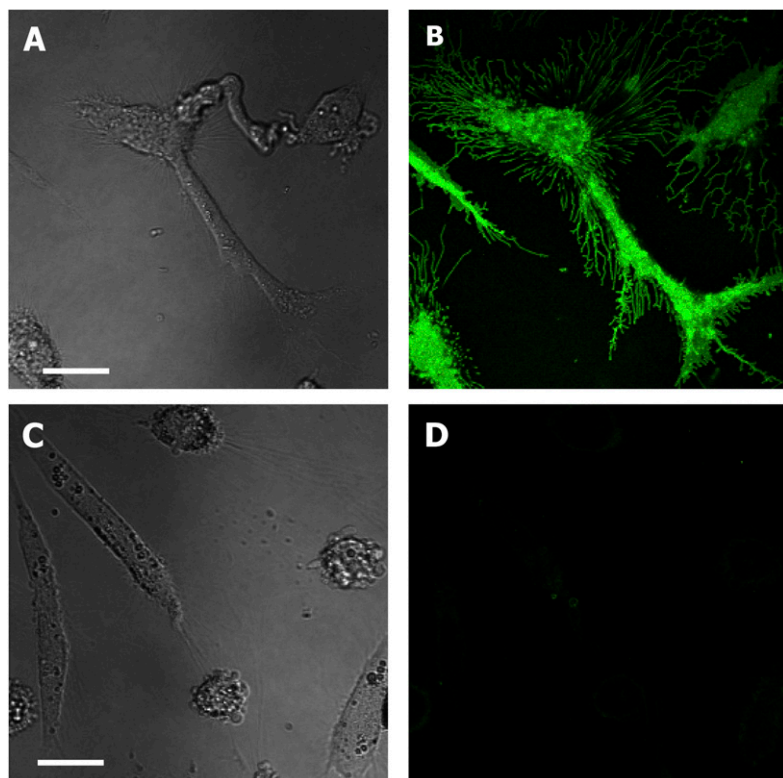


Fig. 4. Performance of C-laurdan and laurdan in confocal microscopy. Images of melanophore cells labeled under identical conditions with either C-laurdan (A, B) or laurdan (C, D) were acquired in the confocal microscope, registering simultaneously the transmitted light (A–C) and the fluorescence intensity in channel 1 (B–D). The look-up table used in B and D was the same. Bar = 10 μm.

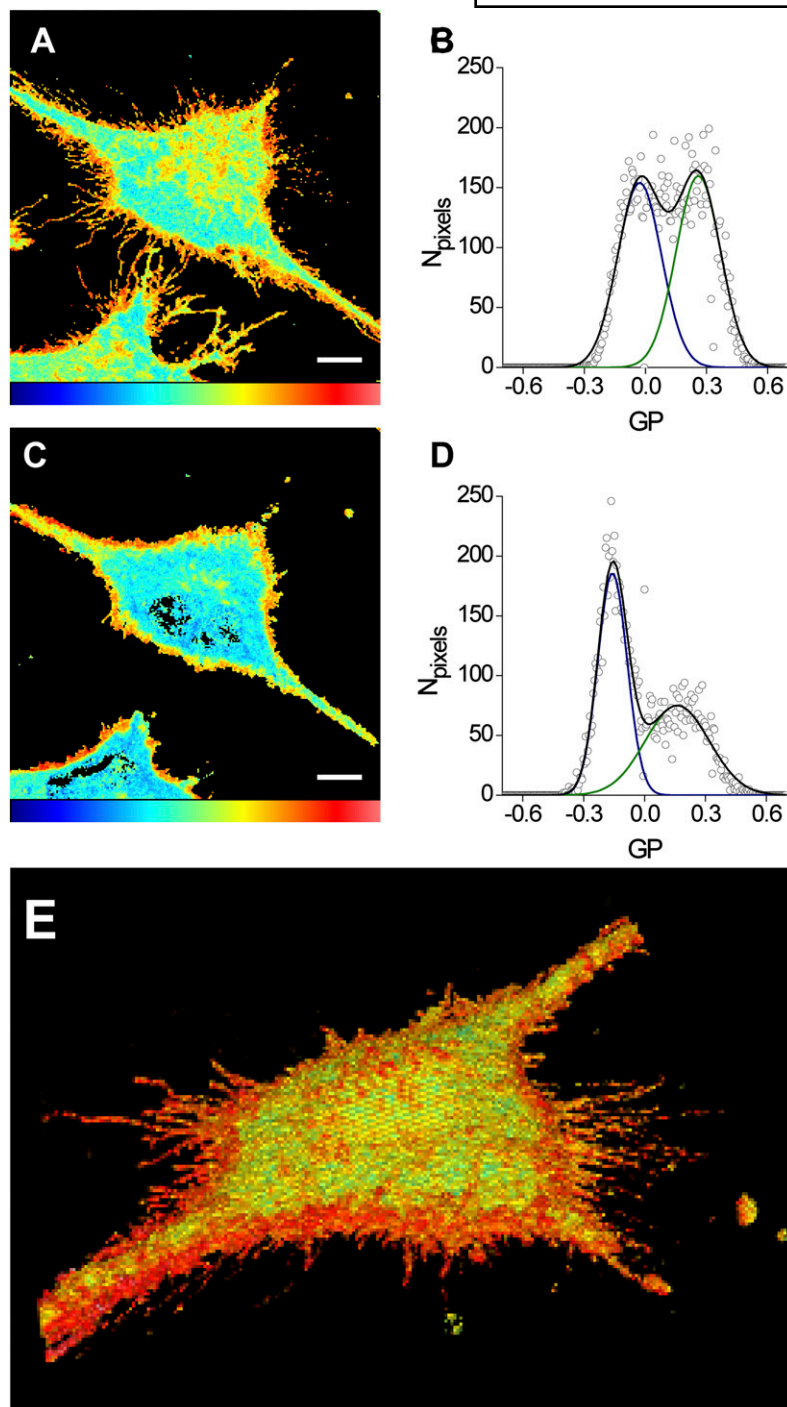


Fig. 5. Observation of lipid order in cellular membranes with C-laurdan. GP images of living cells were obtained as described previously at the basal membrane of the cell (A) and 2.8 μm above the glass support (C). The global distribution of GP at the two planes (B and D, respectively) was fitted with the sum of two Gaussian functions, obtaining the following values for the parameters: $\text{GP}_1 = -0.028 \pm 0.009$; $\sigma_1 = 0.107 \pm 0.008$; $\text{GP}_2 = 0.260 \pm 0.009$; $\sigma_2 = 0.109 \pm 0.008$ (B), and $\text{GP}_1 = -0.157 \pm 0.002$; $\sigma_1 = 0.072 \pm 0.002$; $\text{GP}_2 = 0.161 \pm 0.009$; $\sigma_2 = 0.158 \pm 0.009$ (D). Bar = 10 μm . Three-dimensional reconstruction of the central cell obtained from a stack composed of 21 images acquired at a z-interval of 0.4 μm . The image was created with the ImageJ 3D viewer plugin (E).

Supplementary Fig. V shows C-laurdan GP images of control and MbCD-treated *X. laevis* melanophores at middle planes of the cells obtained with the confocal microscope. We used a Matlab routine to distinguish the cell membrane from the cytoplasm and calculated histograms of GP at the cell membrane before and after the addition of MbCD. The figure illustrates that C-laurdan GP significantly decreases after treatment with MbCD, showing that this probe can efficiently sense changes in membrane fluidity. The average GP values obtained at the cellular membrane were 0.18 ± 0.05 (N cells = 12) and -0.06 ± 0.08 (N cells = 13) before and after the treatment, respectively. Agreeing with our data,

Kim et al. (22) verified that C-laurdan GP values measured in A431 cells significantly decreased after treatment with MbCD using two-photon excitation conditions.


These results show that C-laurdan allows a clear evaluation of regions with different fluidity properties in biological membranes, and thus it can be successfully used to study membrane organization in living cells.

FINAL REMARKS

Laurdan is one of the fluorescent probes most widely used to study lateral organization of membranes in either

artificial or natural systems. Despite its exquisite ability to sense the polarity of the environment, its low photostability has limited enormously the applications of the probe in biological studies. The probe can only be used for imaging under two-photon excitation conditions and the actual high cost of two-photon microscopes is a main limitation for most research groups that may want to include laurdan in their studies.

In this work, we studied the performance of the fluorescent probe C-laurdan for imaging natural and artificial lipid systems under one-photon excitation conditions in a conventional confocal microscope. Surprisingly, we found that the fluorescent probe allows the imaging of biological membranes under typical imaging conditions and low probe concentrations. Moreover, we found that the bathochromic shift of the probe can be easily evaluated under these conditions by using the GP function, thus allowing the study of the lateral organization of membranes without the need of the very expensive two-photon excitation microscope required for laurdan GP measurements. Also, we verified that the photobleaching of the probe was not a limitation for imaging under our experimental conditions.

Because this fluorescence probe can be used with a conventional confocal microscope setup, we believe that the use of this probe will expand the possibility of performing studies of membrane organization and dynamics to research groups all over the world. 

The authors are grateful to Prof. Bong Rae Cho for kindly providing us with C-Laurdan. We are also grateful to Dr. Alejandra Tricerri and Dr. Dolores Carrer for kindly providing us with MbCD and DOPC/SPM, respectively. We also thank Carla Pallavicini for helping us with the Matlab routine and Susana Sanchez for helpful discussion.

REFERENCES

- Simons, K., and M. J. Gerl. 2010. Revitalizing membrane rafts: new tools and insights. *Nat. Rev. Mol. Cell Biol.* **11**: 688–699.
- Jacobson, K., O. G. Mouritsen, and R. G. Anderson. 2007. Lipid rafts: at a crossroad between cell biology and physics. *Nat. Cell Biol.* **9**: 7–14.
- Lingwood, D., and K. Simons. 2010. Lipid rafts as a membrane-organizing principle. *Science*. **327**: 46–50.
- Zech, T., C. S. Ejsing, K. Gaus, B. de Wet, A. Shevchenko, K. Simons, and T. Harder. 2009. Accumulation of raft lipids in T-cell plasma membrane domains engaged in TCR signalling. *EMBO J.* **28**: 466–476.
- Miguel, L., D. M. Owen, C. Lim, C. Liebig, J. Evans, A. I. Magee, and E. C. Jury. 2011. Primary human CD4⁺ T cells have diverse levels of membrane lipid order that correlate with their function. *J. Immunol.* **186**: 3505–3516.
- Klemm, R. W., C. S. Ejsing, M. A. Surma, H.-J. Kaiser, M. J. Gerl, J. L. Sampaio, Q. de Robillard, C. Ferguson, T. J. Proszynski, A. Shevchenko, et al. 2009. Segregation of sphingolipids and sterols during formation of secretory vesicles at the trans-Golgi network. *J. Cell Biol.* **185**: 601–612.
- Schuck, S., and K. Simons. 2004. Polarized sorting in epithelial cells: raft clustering and the biogenesis of the apical membrane. *J. Cell Sci.* **117**: 5955–5964.
- Brügger, B., B. Glass, P. Haberkant, I. Leibrecht, F. T. Wieland, and H.-G. Kräusslich. 2006. The HIV lipidome: a raft with an unusual composition. *Proc. Natl. Acad. Sci. USA*. **103**: 2641–2646.
- Saad, J. S., J. Miller, J. Tai, A. Kim, R. H. Ghanam, and M. F. Summers. 2006. Structural basis for targeting HIV-1 Gag proteins to the plasma membrane for virus assembly. *Proc. Natl. Acad. Sci. USA*. **103**: 11364–11369.
- Takeda, M., G. P. Leser, C. J. Russell, and R. A. Lamb. 2003. Influenza virus hemagglutinin concentrates in lipid raft microdomains for efficient viral fusion. *Proc. Natl. Acad. Sci. USA*. **100**: 14610–14617.
- Lasic, D. D. 1988. The mechanism of vesicle formation. *Biochem. J.* **256**: 1–11.
- Bangham, A. D., M. M. Standish, and J. C. Watkins. 1965. Diffusion of univalent ions across the lamellae of swollen phospholipids. *J. Mol. Biol.* **13**: 238–252.
- Richer, R. P., R. Bérat, and A. R. Brisson. 2006. Formation of solid-supported lipid bilayers: an integrated view. *Langmuir*. **22**: 3497–3505.
- Castellana, E. T., and P. S. Cremer. 2006. Solid supported lipid bilayers: from biophysical studies to sensor design. *Surf. Sci. Rep.* **61**: 429–444.
- Walde, P., K. Cosentino, H. Engel, and P. Stano. 2010. Giant vesicles: preparations and applications. *ChemBioChem*. **11**: 848–865.
- Bagatolli, L. A., and E. Gratton. 1999. Two-photon fluorescence microscopy observation of shape changes at the phase transition in phospholipid giant unilamellar vesicles. *Biophys. J.* **77**: 2090–2101.
- Weber, G., and F. J. Farris. 1979. Synthesis and spectral properties of a hydrophobic fluorescent probe: 6-propionyl-2-(dimethylamino) naphthalene. *Biochemistry*. **18**: 3075–3078.
- Parasassi, T., E. K. Krasnowska, L. Bagatolli, and E. Gratton. 1998. Laurdan and prodan as polarity-sensitive fluorescent membrane probes. *J. Fluoresc.* **8**: 365–373.
- Viard, M., J. Gallay, M. Vincent, O. Meyer, B. Robert, and M. Paternostre. 1997. Laurdan solvatochromism: solvent dielectric relaxation and intramolecular excited-state reaction. *Biophys. J.* **73**: 2221–2234.
- Sánchez, S. A., M. A. Tricerri, G. Ossato, and E. Gratton. 2010. Lipid packing determines protein-membrane interactions: challenges for apolipoprotein A-I and high density lipoproteins. *Biochim. Biophys. Acta*. **1798**: 1399–1408.
- Bagatolli, L. A., and E. Gratton. 2001. Direct observation of lipid domains in free-standing bilayers using two-photon excitation fluorescence microscopy. *J. Fluoresc.* **11**: 141–160.
- Kim, H. M., H. J. Choo, S. Y. Jung, Y. G. Ko, W. H. Park, S. J. Jeon, C. H. Kim, T. Joo, and B. R. Cho. 2007. A two-photon fluorescent probe for lipid raft imaging: C-laurdan. *ChemBioChem*. **8**: 553–559.
- Yi, J.-S., H.-J. Choo, B.-R. Cho, H.-M. Kim, Y.-N. Kim, Y.-M. Ham, and Y.-G. Ko. 2009. Ginsenoside Rh2 induces ligand-independent Fas activation via lipid raft disruption. *Biochem. Biophys. Res. Commun.* **385**: 154–159.
- Huang, C.-H. 1969. Phosphatidylcholine vesicles. Formation and physical characteristics. *Biochemistry*. **8**: 344–352.
- Koynova, R., and M. Caffrey. 1998. Phases and phase transitions of the phosphatidylcholines. *Biochim. Biophys. Acta*. **1376**: 91–145.
- Angelova, M. I., and D. S. Dimitrov. 1986. Liposome electroformation. *Faraday Discuss.* **81**: 303–311.
- Bagatolli, L. A., S. A. Sanchez, T. Hazlett, and E. Gratton. 2003. Giant vesicles, Laurdan, and two-photon fluorescence microscopy: evidence of lipid lateral separation in bilayers. *Methods Enzymol.* **360**: 481–500.
- Parasassi, T., E. Gratton, W. M. Yu, P. Wilson, and M. Levi. 1997. Two-photon fluorescence microscopy of laurdan generalized polarization domains in model and natural membranes. *Biophys. J.* **72**: 2413–2429.
- Korlann, Y., T. Dertinger, X. Michalet, S. Weiss, and J. Enderlein. 2008. Measuring diffusion with polarization-modulation dual-focus fluorescence correlation spectroscopy. *Opt. Express*. **16**: 14609–14616.
- Amos, W. B., S. Reichelt, D. M. Cattermole, and J. Laufer. 2003. Re-evaluation of differential phase contrast (DPC) in a scanning laser microscope using a split detector as an alternative to differential interference contrast (DIC) optics. *J. Microsc.* **210**: 166–175.
- Rogers, S. L., I. S. Tint, P. C. Fanapour, and V. I. Gelfand. 1997. Regulated bidirectional motility of melanophore pigment granules along microtubules in vitro. *Proc. Natl. Acad. Sci. USA*. **94**: 3720–3725.
- Parasassi, T., G. De Stasio, G. Ravagnan, R. M. Rusch, and E. Gratton. 1991. Quantitation of lipid phases in phospholipid vesicles by the generalized polarization of Laurdan fluorescence. *Biophys. J.* **60**: 179–189.
- Parasassi, T., and E. Gratton. 1995. Membrane lipid domains and dynamics as detected by Laurdan fluorescence. *J. Fluoresc.* **5**: 59–69.

34. Sanchez, S. A., L. A. Bagatolli, E. Gratton, and T. L. Hazlett. 2002. A two-photon view of an enzyme at work: *Crotalus atrox* venom *pla2* interaction with single-lipid and mixed-lipid giant unilamellar vesicles. *Biophys. J.* **82**: 2232–2243.
35. Bagatolli, L. A. 2006. To see or not to see: lateral organization of biological membranes and fluorescence microscopy. *Biochim. Biophys. Acta.* **1758**: 1541–1556.
36. Bagatolli, L. A., and E. Gratton. 2000. Two photon fluorescence microscopy of coexisting lipid domains in giant unilamellar vesicles of binary phospholipid mixtures. *Biophys. J.* **78**: 290–305.
37. Li, L., and J. X. Cheng. 2006. Coexisting stripe- and patch-shaped domains in giant unilamellar vesicles. *Biochemistry.* **45**: 11819–11826.
38. Shoemaker, S. D., and T. K. Vanderlick. 2003. Material studies of lipid vesicles in the L(α) and L(α)-gel coexistence regimes. *Biophys. J.* **84**: 998–1009.
39. Baumgart, T., G. Hunt, E. R. Farkas, W. W. Webb, and G. W. Feigenson. 2007. Fluorescence probe partitioning between Lo/Ld phases in lipid membranes. *Biochim. Biophys. Acta.* **1768**: 2182–2194.
40. Gaus, K., E. Gratton, E. P. W. Kable, A. S. Jones, I. Gelissen, L. Kritharides, and W. Jessup. 2003. Visualizing lipid structure and raft domains in living cells with two-photon microscopy. *Proc. Natl. Acad. Sci. USA.* **100**: 15554–15559.
41. Gaus, K., S. Le Lay, N. Balasubramanian, and M. A. Schwartz. 2006. Integrin-mediated adhesion regulates membrane order. *J. Cell Biol.* **174**: 725–734.
42. Sanchez, S. A., G. Gunther, M. A. Tricerri, and E. Gratton. 2011. Methyl-beta-cyclodextrins preferentially remove cholesterol from the liquid disordered phase in giant unilamellar vesicles. *J. Membr. Biol.* **241**: 1–10.
43. Sanchez, S. A., M. A. Tricerri, and E. Gratton. 2007. Interaction of high density lipoprotein particles with membranes containing cholesterol. *J. Lipid Res.* **48**: 1689–1700.